SPS/DI/LT/EJNW/b1

15th November, 1976

Mlle Susan LEECH/Bib.SPS
Commissioning = 2 ex.

SPS Commissioning Report No. 30

Topic : Accelerating More Than 10^{13} Protons in the SPS at 200 GeV and at 400 GeV

Experimenters : D. Boussard, M. Cornacchia, P. Faugeras, R. Lauckner, T. Linnecar, A. Millich, W. Mills, J.C. Soulié, R. Stiening and E.J.N. Wilson

Date : 25 October 1976 (200 GeV) - 3 November 1976 (400 GeV) .

---

1. Introduction

On the afternoon of 25th October 1976, the SPS first reached its design intensity by accelerating 10^{13} protons to 200 GeV (Figure 1). Stable operating conditions were established in which accelerated beam consistently exceeded this figure, occasionally reaching 1.2×10^{13} p.p.p. On the night of 3rd November the design intensity was reached at 400 GeV.

2. Two Pulse Injection from the CPS

Earlier runs had shown that even when the CPS accelerates somewhat more than 10^{13} protons one cannot hope to sustain an operational situation in which 10^{13} protons circulate at 10 GeV in the SPS. The theoretical efficiency of the continuous transfer extraction is not above 90% and the vertical emittance of the beam reaching the SPS can only be kept within the acceptance by careful tuning of both machines. It became clear that to sustain the design intensity we would have to load more than one CPS pulse before accelerating in the SPS at the cost of an extension of the cycle time of 1.2 seconds, the interval between CPS pulses. Improvements in CPS intensity now being tested may later allow us to reach 10^{13} with a single injected pulse.

This two-pulse mode of injection was tested for the first time on 25th October. Each of the two CPS pulses contained almost 10^{13} protons and was transferred to fill half the SPS circumference with the CPS continuous transfer kickers set to extract over five CPS turns rather than the ten needed to fill the SPS.

Five-turn transfer of single pulses had been tried in the past and we had observed that the SPS was if anything less prone to certain longitudinal instabilities. We had also suppressed the resistive wall (Ref. 1) and head-tail instability (Ref. 2) with this mode of transfer and hoped that if it did not provide an easier route to the design intensity we would at least learn more about the SPS and its limits.

In order to inject the second CPS pulse in the empty half left in the SPS ring after the injection of the first CPS batch, one has synchronized the CPS extraction system and the SPS injection kicker in the following way: once the first CPS batch is injected and trapped in the RF buckets, the clock pulses at the SPS revolution frequency generated by the RF system are locked in phase with the hole of the circulating beam. These clock pulses are sent back to the CPS and are used to trigger 1.2 sec later the second transfer from the CPS, which in turn triggers the SPS inflector.

Figure 2 shows the resulting circulating beam as well as the kick pulse applied to the second CPS batch. The comparison of the waveform of the first CPS batch before the second kick and after it on the following turns shows that this batch is not perturbed by the second injection. Similarly one can see that the second batch is injected without losses.

Rough measurements of the width of the holes in the circulating beam were made by changing slightly the time at which the second kick pulse is triggered, as well as its pulse duration. One has found: batch 1 - batch 2 : 1.2 μs $\pm$ 0.2; batch 2 - batch 1 : 0.8 μs $\pm$ 0.2.

This double injection scheme has been proved to be effective and reliable when the intensity per injected batch was raised to $8 - 9.10^{12}$ ppp.

3. RF Capture of the Two Pulses

The major tasks of the RF system in the double injection scheme are:

(1) to prevent the first batch of injected protons from swerving out into the empty half of the circumference because of their energy spread and

(2) to keep the longitudinal quality of the first batch from deteriorating during the 1.2 sec wait-time between the two injections.

The procedure adopted was as follows:

(a) The first injected batch was left to debunch its 9.5 MHz structure during 100 msec. Then, the RF voltage was slowly turned on and the batch adiabatically captured into 200 MHz buckets.

(b) The first batch was thus kept by the RF beam control during the wait-time at constant B field. Then the RF voltage was lowered adiabatically from 2.2 MV down to about 100 KV (thus minimizing the longitudinal blow up) and then switched off abruptly a few milliseconds before the second injection.

(c) After injection of the second batch in the empty half of the circumference, the RF was kept off for 100 msec so that both the 9.5 MHz and the 200 MHz structures in the beam would disappear. Then the entire beam was adiabatically captured and accelerated in the normal way. In spite of the RF gymnastics which half of the beam had undergone, the overall capture efficiency turned out to be as good as 90%, which is very close to the efficiency one has with simple injection (Figure 3).

4. The Magnet Cycle

A special power supply cycle (Figure 4) was used with a 800 msecond rest time after descent to 10 GeV to allow eddy current and remanent field effects to subside in the guide field (Reference 3). This was followed by a 1400 msecond injection platform to allow injection of the two CPS pulses. There was still time within the 6 second supercycle to accelerate to 200 GeV leaving a flat top. Previous experiments (Reference 4) had shown that Q values of 27.42 horizontally and 27.38 vertically gave better transmission than the nominal 27.6 working point which lies on a system of fifth order systematic stop-bands. The lower working point was used throughout the run, a decision which proved prudent in the light of a subsequent unsuccessful attempt to reach 10^{13} at the upper working point.

5. Tuning Transverse Dynamics

After double-pulse injection had been set up and standard tuning procedures applied to minimise injection oscillations and closed orbit excursions, we trimmed Q throughout the cycle to stay close to the desired Q values.

The injection chromaticity was adjusted with the chromaticity sextupoles to give maximum coherent ringing of betatron oscillations and then made slightly negative to suppress the head-tail instability below transition.

The active betatron dampers were optimised to prevent resistive wall instability and the harmonic quadrupole correctors set to values which had compensated the neighbouring half integer stop-bands in a previous experiment (Reference 5). This was the first time these quadrupoles had been used in a high-intensity run. Skew quadrupoles were powered to the settings which compensate the main diagonal coupling resonance (Reference 6).

At this moment a rapidly growing instability was seen between 50 and 100 GeV. We found its onset could be delayed by applying strong positive chromaticity correction in the horizontal plane with the chromaticity sextupoles at full current. By ramping the Landau damping octupoles to full strength from their injection level of 2 amps we were able to prevent the instability altogether. This behaviour is consistent with a horizontal manifestation of the head-tail instability.

6. Reaching the Design Intensity

We describe the details of the 200 GeV run; the 400 GeV run was essentially similar.

Since only a modest loss during the parabola remained, we asked the CPS for full intensity and very soon observed some pulses which exceeded the design intensity at 200 GeV. The machine was clearly better tuned than ever before and even when the occasional misfire resulted in only one pulse reaching the SPS the accelerated current exceeded the previous best of 5×10^{12}.

Figure 5 shows an intensity balance sheet with the two CPS pulses appearing in two columns and three samples of the SPS beam just before and just after the second pulse is injected and again at 200 GeV. The units are 10^{10} protons.

We went on to reduce losses in the early part of the cycle by tuning Q_H in the parabola. There appears to be an acceptance waist in this region. A peak circulating beam at 200 GeV of 1.2×10^{13} is shown digitised at 20 ms intervals in Figure 6. At this time the CPS was sending two pulses of 9×10^{12} into TT10 of which 1.4×10^{13} protons circulated at 10 GeV in the SPS.

Conditions stabilised with more than 10^{13} protons at 200 GeV on all but a few weak pulses. Even when the power supply was switched off, reloaded with a different cycle and following another experiment reloaded again, the SPS came back very quickly to more than 10^{13} per pulse.

During the subsequent 400 GeV run, it became clear that it was only just possible to stabilise the head-tail instability at high energy at 10^{13} protons per pulse. Full damping octupole current was used.

Acknowledgement

We would like to thank the SPS Operations Group and the CPS staff who responded promptly and imaginatively to our request for two-pulse operation and who, by providing a stable full intensity beam over many hours, made these experiments possible.

References

1. SPS Commissioning Report No. 17 - Bossart, Stiening and Wilson - Vertical Beam Damper.

2. SPS Commissioning Report No. 26 - Cornacchia, Mills, Lauckner and Wilson - The Head-Tail Effect and its Suppression in the SPS.

3. SPS Commisioning Report No. 29 - Linnecar, Mills, Lauckner, Stiening and Wilson - Guide-Field Draft following Descent to 10 GeV/c.

4. SPS Commissioning Report No. 28 - Cornacchia, Lauckner, Mills, Stiening and Wilson - The Transverse Acceptance of the SPS at Injection.

5. SPS Commissioning Report No. 27 - The Correction Elements Working Group - Correction of Half-Integer Resonances at Injection.

6. SPS Commissioning Report No. 24 - Myae, Stiening and Wilson - Measurement and Compensation of Radial-Vertical Betatron Coupling.

---

25 OCTOBER 1976

15.54

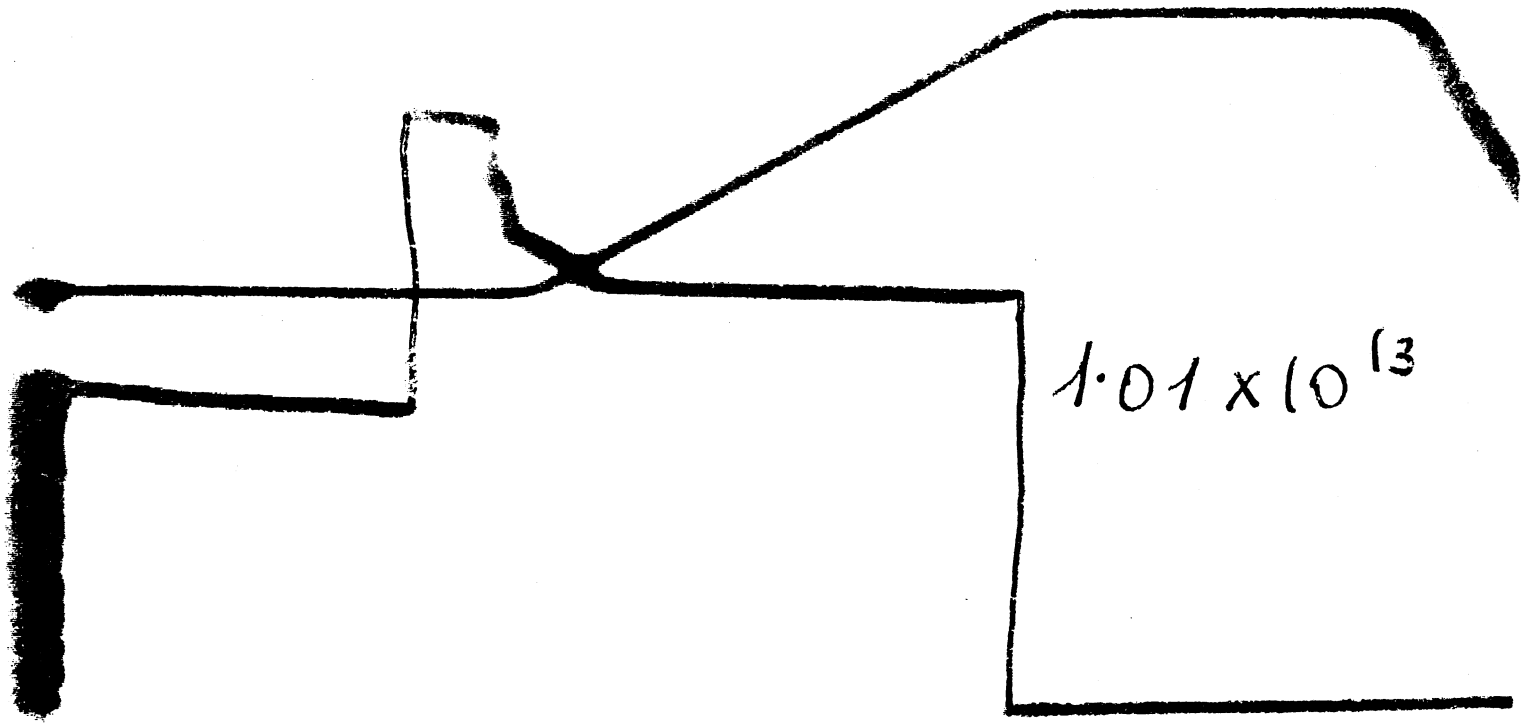

66628

Figure 1

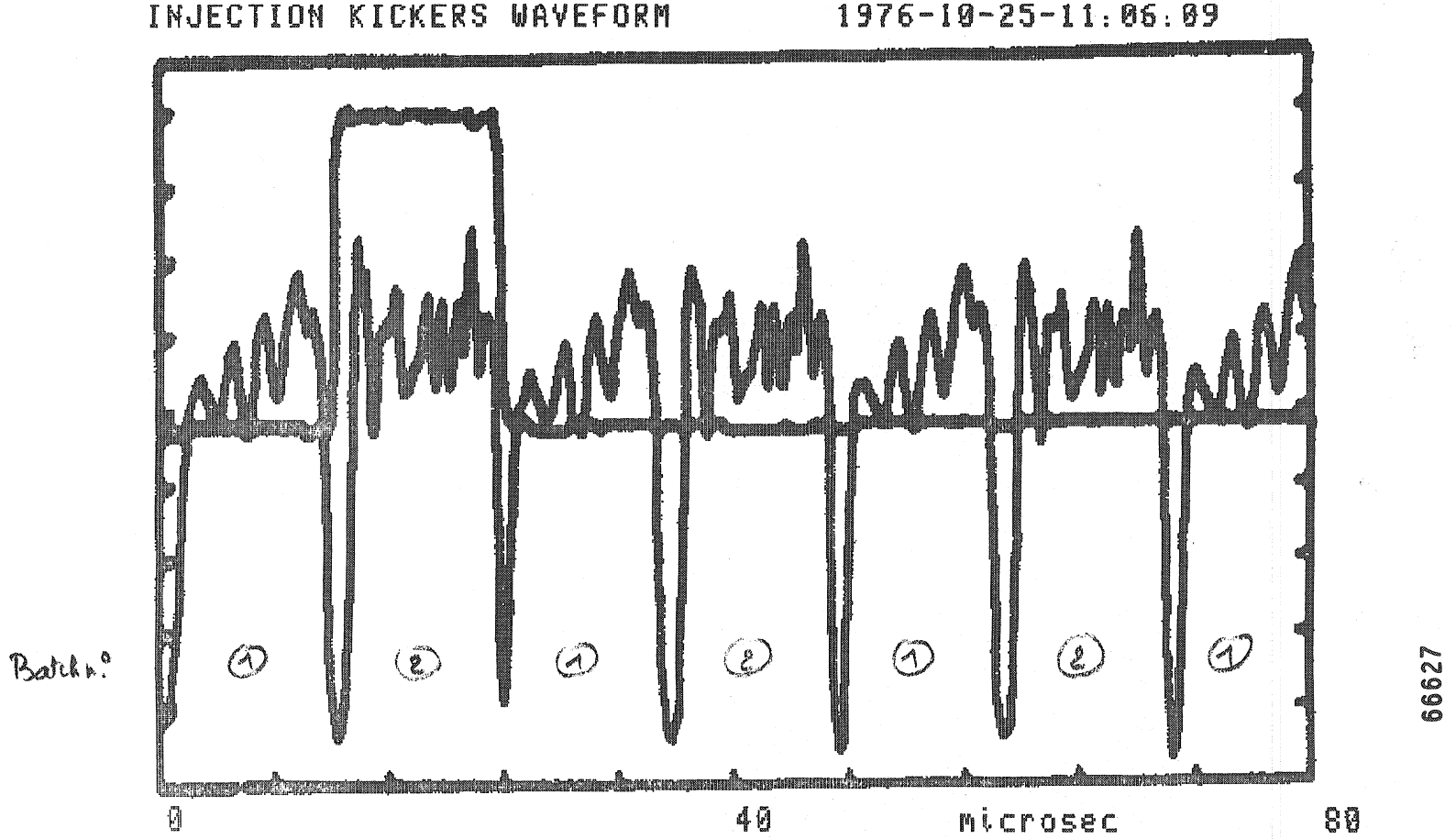
INJECTION KICKERS WAVEFORM
1976-10-25-11:06:09
Batch n°
1
2
1
2
1
2
1
0
40
microsec
80
Kick No.1 - PFN Charging Voltage 34.87 KV
CHANNEL 1 : MKI 1 Term. Resistor
CHANNEL 2 : Injected Beam Current (+ve)
66627

Figure 2

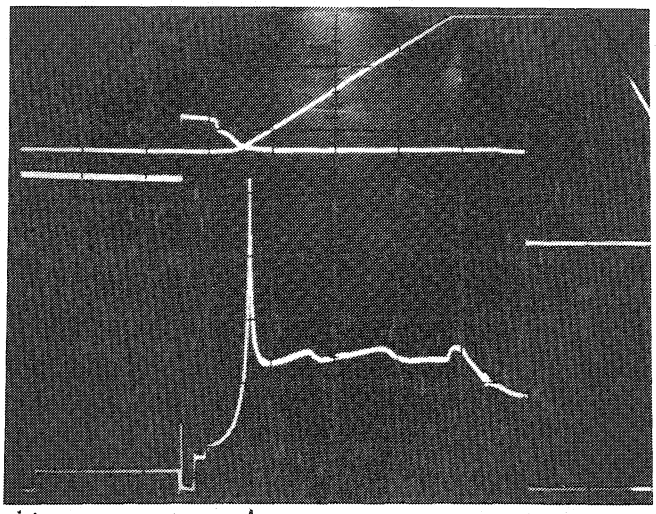

66626

Note that the capture efficiency is about 90%. Untrapped particles correspond to the abrupt beam loss at the beginning of the parabola.

Figure 3

1976-10-25-17:39:29	ACTIVE CYCLE	NEW CYCLE
B STATIONS SELECTED	111111 111111	111111 111111
NO. OF SUBCYCLES	1	1
QH	27.420	27.420
QV	27.380	27.380
INJECTION, GEV/C	10.037	10.037
DEBUNCHING TIME, S	1.440	1.440
FRONT PORCH TYPE	1	1
NO. OF FLAT TOPS	1	1
FLAT TOP 1, GEV/C		
FLAT TOP 1 TIME, S		
FLAT TOP 2, GEV/C	200.0	200.0
FLAT TOP 2 TIME, S	1.020	1.020
TOTAL CYCLE TIME, S	6.000	6.000
DEAD TIME, S	.840	.840
RMS CURRENT) B	41.9	41.9
% OF MAX.) QF	39.7	39.7
QD	39.7	39.7
FILENAME		<77>CYCLE1

66623

Figure 4

```
TT10 BEAM STATUS <61>TTSTAT              1976-10-25-17:43:

IPP    933 971        PS CIRCULATING CURRENT (10^10 PPP)
IEX    870 893        PS EXTRACTED BEAM CURRENT
IN1    824 860        TT10  UPNSTREAM CURRENT (0, 1200 MSEC)
IN2    821 847        TT10 DOWNSTREAM CURRENT (0, 1200 MSEC)
IR1    70913911107    CIRCULATING CURRENT (1180,1220,3000 MSEC)

BEX   4771 4772       PS FIELD AT EXTRACTION(GAUSS)
RFV     36            PS RF VOLTAGE (KILOVOLTS)
RFM   1102            PS RF MODULATION @ (200MHZ)
STP     79            NUMBER OF STOPS
```

66625

Figure 5

BEAM CURRENT IN 20 MILLISECONDS 25 OCTOBER 1976 23.56

0	767	761	751	764	765	760	757	757	760	754
200	752	753	756	748	742	744	750	750	745	745
400	746	745	744	742	746	747	742	738	743	745
600	739	734	737	741	740	736	738	741	738	732
800	733	732	735	731	729	733	736	730	728	730
1000	732	729	725	728	732	729	724	724	728	729
1200	-1414	-1414	-1414	-1414	-1414	-1414	-1414	-1414	-1414	-1414
1400	-1414	-1414	-1415	-1425	1388	1368	1359	1351	1346	1342
1600	1337	1328	1319	1308	1300	1293	1286	1284	1273	1263
1800	1258	1255	1252	1250	1247	1246	1243	1245	1246	1246
2000	1245	1245	1247	1245	1245	1246	1245	1247	1246	1245
2200	1245	1243	1245	1244	1245	1245	1245	1246	1248	1245
2400	1245	1245	1245	1246	1245	1245	1245	1244	1243	1243
2600	1244	1243	1243	1245	1246	1247	1246	1246	1245	1244
2800	1245	1245	1244	1245	1244	1244	1243	1243	1242	1243
3000	1244	1245	1244	1245	1245	1246	1245	1245	1245	1246
3200	1246	1245	1243	1243	1243	1245	1244	1245	1244	1245
3400	1245	1246	1245	1245	1244	1244	1241	1242	1242	1243
3600	1243	1244	1244	1243	1242	1242	1240	1239	1237	1236
3800	1232	1236	1236	1236	1236	1235	1234	1233	1232	1230
4000	1230	1231	1229	1226	1225	1225	1225	1224	1224	1223
4200	1222	1224	1221	1219	1218	1218	1216	1215	1214	1213

66624

Figure 6